Fullerenes as Novel Acceptors in Photosynthetic Electron Transfer

Hiroshi Imahori*[a] and Yoshiteru Sakata*[a]

Keywords: Fullerenes / Photosynthesis / Porphyrins / Electron transfer / Donor-acceptor interaction / Self-assembled monolayers

We propose a novel strategy using fullerenes for the construction of solar energy conversion systems that mimic the primary electron transfer events in photosynthesis. Redox-active fullerenes such as C_{60} and C_{70} were covalently bound to a porphyrin and the photophysical properties of the resulting compounds were investigated. Regardless of solvent and linkage, the charge-separated state is produced efficiently in zincporphyrin–fullerene dyads, showing that fullerenes are good electron acceptors. The most intriguing characteristic of fullerenes in electron transfer is that they accelerate photoinduced charge separation as well as charge shift and slow down charge recombination, properties that are in sharp contrast with those of conventional two-dimensional aromatic acceptors such as quinones and imides. The peculiar electron transfer properties of fullerenes can be explained by the small reorganization energies, which make it possible to optimize artificial photosynthetic multistep charge separation. A combination of the two strategies, multistep electron transfer and small reorganization energy of fullerenes, has been applied to light energy conversion systems as well as the more complex molecular systems such as triads. Highly efficient photosynthetic multistep electron transfer has been realized at gold electrodes modified with self-assembled monolayers of fullerene-containing molecules. These results will provide new principles and concepts to develop artificial photosynthetic materials as well as molecular devices.

1. Introduction

Solar energy conversion is one of the most attractive topics for the next century, because it has the potential to solve energy and environmental problems. Solar cells that use

Hiroshi Imahori was born in 1961 and studied chemistry at Kyoto University in Kyoto (Japan). He completed his doctorate with Prof. K. Maruyama at Kyoto University on the electron-transfer photochemistry of quinones. From 1990−1992 he was a post-doctoral fellow with Prof. T. Inoue at the Salk Institute for Biological Studies at La Jolla (USA) working on the development of in vitro selection systems of catalytic RNA, ribozyme. In 1992 he joined the group of Prof. Y. Sakata at Osaka University. His current interests involve artificial photosynthesis, photofunctional materials, self-assembled monolayers, and porphyrin−fullerene chemistry.

Yoshiteru Sakata received his BS (1962), MS (1964), and Ph.D. (1969) in organic chemistry from Osaka University under the guidance of Prof. M. Nakagawa. He joined the group of Prof. S. Misumi at The Institute of Scientific and Industrial Research, Osaka University in 1966. After working at the University of Cologne as an Alexander von Humboldt fellow with Prof. Vogel from 1971 to 1973, he was promoted to Associate Professor (1973) and Full Professor (1991). His current interests cover the relationship between structure and properties of organic compounds and especially focus on photosynthetic electron transfer.

MICROREVIEWS: This feature introduces the readers to the authors' research through a concise overview of the selected topic. Reference to important work from others in the field is included.

---

[a] The Institute of Scientific and Industrial Research,
Osaka University,
Mihoga-oka, Ibaraki, Osaka 567-0047, Japan
Fax: (internat.) +81-6/6879-8479
E-mail: imahori@sanken.osaka-u.ac.jp
sakata@sanken.osaka-u.ac.jp

1434−193X/99/1010−2445 $ 17.50+.50/0

semiconductors such as silicons are available commercially. However, these systems are not ideal with respect to the economic cost as well as the energy conversion efficiency. On the other hand, photosynthesis is one of the most elaborate processes in nature.[1] It converts solar energy into chemical energy, which is essential for living organisms on the earth. The core of photosynthesis is photoinitiated multistep electron transfer between donors and acceptors in the reaction center. Thus, visible light is harvested by the antenna complexes, including chlorophylls and carotenoid polyenes, and the collected energy is funneled into the chlorophyll dimer (special pair) in the reaction center. The subsequent multistep electron transfer takes place unidirectionally along the well-arranged chromophores that are embedded in the transmembrane protein in the sequence of dimer, pheophytin, and quinone. This process produces a charge-separated state across the membrane with a quantum efficiency of nearly 100%. The unique three-dimensional structure and the novel function as solar energy conversion system have fascinated many organic chemists during the last two decades. Organic synthesis allows us to control the electron transfer process by linking donors and acceptors with covalent bonds instead of using the proteins. Therefore, toward the final goal of solar energy conversion, donor-acceptor linked molecules have been prepared to understand the controlling factors for photosynthetic electron transfer.[2−7] In this microreview we will describe a novel approach using fullerenes for the construction of artificial photosynthetic mimics and materials. Fullerenes have been shown to be good acceptors in electron transfer through our studies and other important works.

2. Concept

In donor-acceptor linked dyads (two chromophores), it seems possible to generate a long-lived charge-separated state by tuning the electronic coupling between the donor and the acceptor, i.e. the length and the nature of spacers. However, there is a serious problem in this approach. In general, the coupling decreases in strength as the number of bonds connecting the donor and acceptor increases. Thus, the forward electron transfer rate decreases as the length of spacers increases, resulting in the decreased efficiency in the production of the charge-separated state. In contrast, both the forward and reverse electron transfer rates increase with a decrease of the spacer lengths so that the lifetime of the charge-separated state decreases. Natural photosynthesis has solved the dilemma by employing a multistep electron transfer strategy. Sakata and Mataga et al. suggested a model for photosynthetic multistep electron transfer in 1981.[8] They reported the first synthesis and photophysical properties of donor-acceptor linked triad **1** consisting of a porphyrin (S)-tethered to two quinones (A_1 and A_2) (Figure 1).[9] The energy gradients of each state in the triad are in the order of $^1S^*-A_1-A_2 > S^{\bullet+}-A_1^{\bullet-}-A_2 > S^{\bullet+}-A_1-A_2^{\bullet-}$. Therefore, the second electron transfer from $A_1^{\bullet-}$ to A_2 will compete with the charge recombination to the ground state, producing $S^{\bullet+}-A_1-A_2^{\bullet-}$ in a total sequence of $^1S^*-A_1-A_2 \rightarrow S^{\bullet+}-A_1^{\bullet-}-A_2 \rightarrow S^{\bullet+}-A_1-A_2^{\bullet-}$. The charges at the larger distance will inhibit rapid recombination, as observed in the primary process in photosynthesis. Actually, the lifetime of $S^{\bullet+}-A_1-A_2^{\bullet-}$, produced by the sequential electron transfer, was found to be much longer compared with that in the corresponding dyad. This implies that the larger separation between $S^{\bullet+}$ and $A_2^{\bullet-}$ is effective in prolonging the lifetime. Since the first demonstration of photosynthetic multistep electron transfer in 1982, a number of reports have been published dealing with the synthesis and photophysical properties of triads.[2−7] Gust and Moore et al. have prepared a variety of carotenoid (D)−porphyrin (S)−quinone (A) triads **2** (Figure 2).[5][10] As they expected, a sequential electron transfer occurs from the excited singlet state of the porphyrin ($^1S^*$) to quinone, then from the carotenoid to the porphyrin cation radical ($S^{\bullet+}$), generating the final charge-separated state ($D^{\bullet+}-S-A^{\bullet-}$) efficiently. The advantage of **2** over **1** is that the relatively rigid spacer allows the triad **2** to take a linear comformation, while the flexible methylene spacer in **1** prevents it from adopting an extended conformation. Therefore, $D^{\bullet+}$ and $A^{\bullet-}$ in the $D^{\bullet+}-S-A^{\bullet-}$ state of **2** are well-separated so that the lifetime is markedly prolonged. This work has been extended to tetrad molecules containing a carotenoid, a porphyrin, and two quinones and pentad molecules containing a carotenoid, two porphyrins, and two quinones.[11] The artificial photosynthetic models of these compounds displayed a high quantum yield with a long lifetime for the final charge-separated state when the free energy changes for each electron transfer are well-tuned depending on the solvents as well as the length and the nature of the spacers [i.e. one of the pentads showed an overall quantum yield of 0.83 (0.60) and a lifetime of 55 μs (200 μs) in $CHCl_3$ (CH_2Cl_2)]. These results clearly demonstrate that photoinduced multistep electron transfer is an effective strategy for the construction of artificial photosynthetic systems.

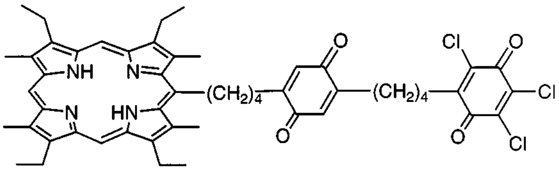

1

Figure 1. Porphyrin−diquinone triad **1** mimicking photoinduced multistep electron transfer in photosynthesis

The major difference between artificial photosynthetic mimics and photosynthesis in nature is that donors and acceptors in the latter are embedded in the protein matrix, while they are generally linked by covalent bonds in the former. On the basis of Marcus theory, the nonadiabatic electron transfer rate constant k_{ET} is expressed by Equation 1, where V is the electronic coupling, $-\Delta G$ is the free energy gap between the equilibrium nuclear configuration of the reactants and the products, λ is the reorganization energy,

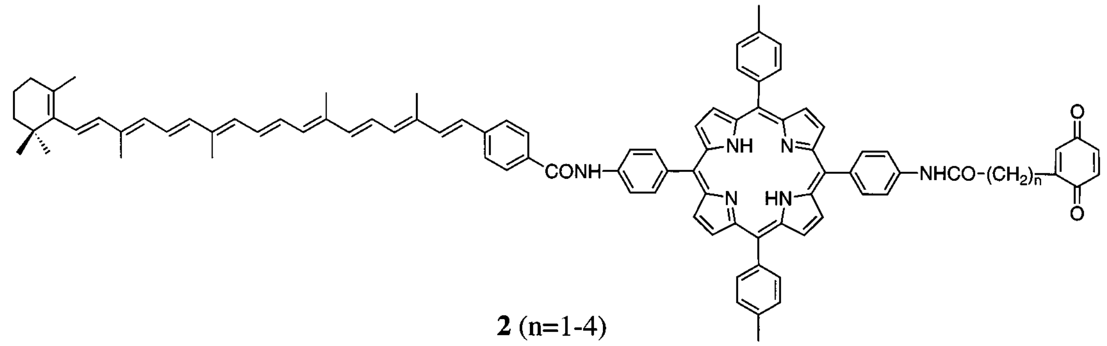

2 (n=1-4)

Figure 2. Carotenoid−porphyrin−quinone triad **2** mimicking photoinduced multistep electron transfer in photosynthesis

T is the absolute temperature, h is Planck′s constant, and k_B is Bolzmann′s constant.[12]

$$k_{ET} = (4\pi^3/h^2\lambda k_B T)^{1/2}\ V^2 \exp[-\Delta G + \lambda)^2/4\lambda k_B T] \qquad (1)$$

The surrounding protein matrix affects not only the electronic coupling between the redox pair, but also the reorganization energy. Let us consider the Marcus parabolic curve for electron transfer. As the free energy change becomes more positive, the electron transfer rate will increase (normal region) until it reaches a maximum point where $-\Delta G = \lambda$ (top region). However, as the free energy change becomes more positive, the electron transfer rate will decrease (inverted region). In photosynthetic electron transfer the value of the reorganization energy is optimized for each electron transfer process. Thus, the forward electron transfer is positioned on the top region so that the process is activationless, whereas it forces the reverse electron transfer to be down a considerable way along the Marcus curve in the inverted region so that the activation barrier for the process is high. Consequently, the forward electron transfer is much faster than the corresponding reverse one in each process, producing the long-lived charge separation with a quantum efficiency of nearly 100%. Actually, the initial electron transfer event of photosynthesis occurs between large π electron systems, which is characterized by a small reorganization energy of 0.2−0.3 eV.[13] In photosynthetic models such as porphyrin−quinone and diporphyrin dyads, the reorganization energies are controlled mainly by the surrounding solvent[14] and the values are near 1 eV in common organic solvents such as dichloromethane.[15] However, synthetic control of reorganization energy due to the intrinsic properties of donors and/or acceptors such as size, shape, heterogeneity of elements, and molecular orbitals, has been considered to be quite difficult. Provided that all the controlling factors, including the free energy change and the electronic coupling, are the same except for the reorganization energy in two donor-acceptor systems, the smaller reorganization energy will make the forward and reverse electron processes faster and slower than the other, respectively. Application of this approach together with multistep electron transfer strategy will make it possible to significantly improve the final quantum yield, lifetime of the charge-separated state, and the amount of energy stored in the system, balancing with the free energy changes and the electronic couplings properly. Accordingly, the development of molecules with small reorganization energy is a matter of vital importance for this purpose. In the following sections we will describe photoinduced accelerated forward electron transfer and decelerated reverse electron transfer in donor-linked fullerenes and their application to light energy conversion systems. It is shown that the peculiar properties of fullerenes in electron transfer are explained by the smaller reorganization energy of fullerenes compared with conventional acceptors such as quinones.

3. Porphyrin−Fullerene Dyads

Porphyrins are the most frequently employed building blocks as electron donors and sensitizers in artificial photosynthetic models. On the other hand, the unique three-dimensional structures of fullerenes, as well as the facile electron acceptability of up to six electrons, make them good candidates as electron acceptors. Therefore, photoinduced electron transfer systems consisting of porphyrins and fullerenes are a good combination for revealing basic electron transfer properties of fullerenes. In the following sections we will focus on photophysical properties of porphyrin−fullerene dyads and triads.

Gust and Moore et al. reported the first preparation and preliminary photophysical properties of porphyrin-linked C_{60}.[16] Imahori and Sakata et al. independently prepared and studied porphyrin (P)-linked C_{60} **3** at the same time (Figure 3).[17] In order to improve the solubility of **3** in common organic solvents, six *tert*-butyl groups were intro-

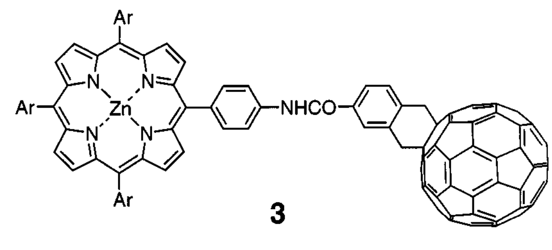

3

Ar=3, 5-(t-Bu)$_2$C$_6$H$_3$

Figure 3. Porphyrin−C_{60} dyad **3**

duced into *meso*-phenyl rings of the porphyrin moiety. C_{60} is covalently attached to a *meso*-porphyrin aryl ring at the *para* position through an amido bond at the final step of the synthesis to avoid tedious purification and characterization caused by the presence of the C_{60}. Ultraviolet-visible absorption spectra and redox potentials of **3** are almost superpositions of those of the single chromophores, indicating that electronic interaction between the two moieties is small.

The first direct evidence for photoinduced electron transfer in donor-linked fullerenes comes from our photophysical studies of **3** using picosecond time-resolved transient absorption spectroscopy (Figure 4).[17] After excitation of the porphyrin in **3**, the $S_n \leftarrow S_1$ absorption corresponding to the porphyrin appeared. As the $S_n \leftarrow S_1$ absorption decayed, a concomitant rise and decay of the transient bands due to the zincporphyrin cation radical ($ZnP^{\bullet +}$) and C_{60} anion radical ($C_{60}^{\bullet -}$) were observed clearly, showing photoinduced electron transfer from the excited singlet state of the porphyrin to the C_{60} in **3**. We have extended this work to include a variety of spacers between the porphyrin and the C_{60} (Figure 5).[18] In addition to **3**, three different kinds of zincporphyrin-linked C_{60} **4−6** have been synthesized by changing systematically the linking position at the *meso*-phenyl ring from *para* to *ortho*. Molecular mechanics calculations predict that **3** takes the extended conformation (R_{cc} = 18.6 Å), whereas **4** (R_{cc} = 14.4 Å) and **5** (R_{cc} = 12.5 Å) adopt chair-like conformations with the closest separation distance between the two chromophores. The C_{60} moiety in **6** is folded onto the porphyrin ring (R_{cc} = 7.6 Å). Regardless of the linkage between the two chromophores, photoinduced charge separation and subsequent charge recombination were observed in a series of zincporphyrin−C_{60} dyads **3−6** by picosecond fluorescence lifetime measurements and time-resolved transient absorption spectroscopy. In THF the charge separation occurs from both the excited singlet state of the porphyrin and the C_{60} moieties, implying that an increase of the absorption cross section by both the chromophores results in the efficient formation of the charge-separated state. In benzene the energy level of the charge-separated state is positioned above that of $ZnP{-}^1C_{60}^*$ or at the near level. Therefore, the charge-separated state in **3** and **4**, generated by the photoinduced charge separation from the excited singlet state of the porphyrin to the C_{60}, recombines to produce $^1C_{60}^*$, while in **5** it energetically equilibrates with $^1C_{60}^*$. Both the charge separation and charge recombination rates for **4** are much slower than those for the other porphyrin-linked C_{60} compounds: **3**, **5**, and **6**. Linkage-dependence of the electron transfer rates can be explained reasonably by the superexchange mechanism by through-bond interaction. Thus, molecular orbital calculations on the linkage show that electron densities at *ortho*- and *para*-positions in the HOMO and LUMO levels are much larger than the values at the *meta*-position. This indicates that electronic coupling between the two chromophores through the *meta*-position is much smaller than for the other two positions, thereby yielding the electron transfer trend.

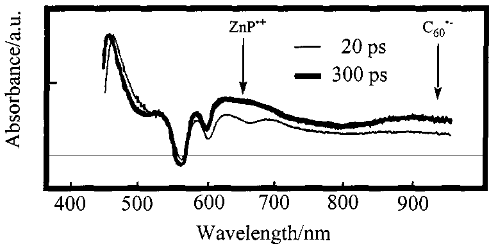

Figure 4. Picosecond time-resolved transient absorption spectra of **1** in THF excited at 590 nm; the spectra are normalized at the Soret band for comparison

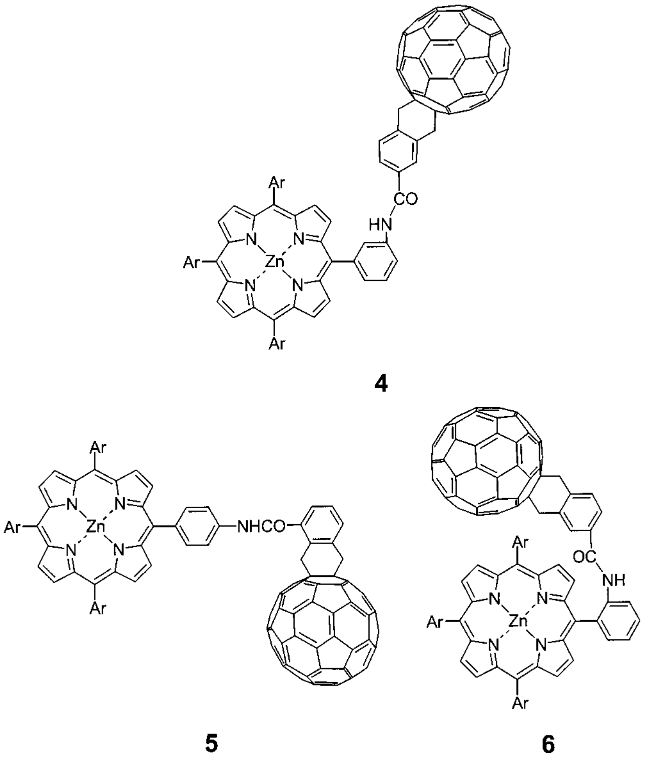

Ar=3, 5-(*t*-Bu)$_2$C$_6$H$_3$

Figure 5. Porphyrin−C_{60} dyads **4−6**

In order to evaluate the intrinsic effect of C_{60} in photoinduced electron transfer, porphyrin-linked quinone **7** has been designed and synthesized (Figure 6).[19] In compound **7** the C_{60} of **3** is replaced by benzoquinone (Q), one of the commonly used acceptors, because Q (−0.45 V vs. Ag/AgCl) has a similar first reduction potential to that of the C_{60} (−0.65 V vs. Ag/AgCl). The quinone is linked to a porphyrin with a semi-rigid spacer, which ensures a similar separation distance and nature of the intervening bonds between the redox pair. In THF the forward electron transfer rate (k_{CS}) of **3** is larger than that of **7** by a factor of 6. On the other hand, the charge recombination rate (k_{CR}) of **3** is smaller by a factor of < 1/25 compared with that of **7**. A similar trend was observed in other solvents such as benzene and DMF.

A number of donor-linked C_{60} dyads have been prepared to date.[16−82] Similar accelerated photoinduced forward

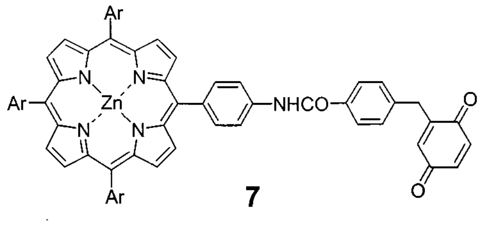

7

Ar=3, 5-(t-Bu)$_2$C$_6$H$_3$

Figure 6. Porphyrin−quinone dyad **7**

electron transfer and decelerated reverse electron transfer have been reported.[21] The ratios of k_{CS}/k_{CR} in donor-linked C_{60} dyads are much higher than those in conventional two-dimensional donor−acceptor dyads such as porphyrin−quinones, porphyrin−imides, diporphyrins, and others. There are two explanations for the outstanding effect of C_{60}. Verhoeven and Paddon-Row et al. reported the large electronic coupling for photoinduced charge separation and the smaller one for charge recombination in donor-linked C_{60}. They propose, based on semiempirical AM1 molecular orbital calculations, that these results are mainly due to the special symmetry properties of the fullerene π system.[45,46,50] Imahori and Sakata et al. proposed that the results could be attributed to the smaller reorganization energy of C_{60} compared with those of typical two-dimensional acceptors.[18,19,21] On the Marcus parabolic curve the small reorganization energy of C_{60} pushes the photoinduced charge separation upward along the normal region into the top region, while it also forces the charge recombination significantly downward into the inverted region. Therefore, the photoinduced electron transfer is accelerated, whereas the reverse electron transfer is retarded. Gust and Moore et al. mentioned that the C_{60} effect must be due to the reorganization energy or the electronic coupling.[22]

Our explanation for the C_{60} effect in electron transfer is that the unit charge in $C_{60}^{\bullet -}$ is highly delocalized over the three-dimensional carbon framework of C_{60}, while the charge in $Q^{\bullet -}$ is concentrated largely on the oxygen atoms. Thus, the charge density of each carbon in $C_{60}^{\bullet -}$ is much smaller than that of $Q^{\bullet -}$, making the solvent reorganization energy (λ_s) of C_{60} smaller. The small Raman and Stokes shifts on reduction and photoexcitation of fullerenes support the rigid structure of C_{60}, where the internal reorganization energy (λ_i) is small.[34][83] Consequently, the total reorganization energy ($\lambda = \lambda_s + \lambda_i$) in C_{60} would be small. Activation energies for the forward electron transfer ($\Delta G^{\neq}{}_{CS}$) and the reverse electron transfer ($\Delta G^{\neq}{}_{CR}$) in **3** are much reduced and increased, respectively, compared with those in **7** as illustrated in Figure 7. Tachiya et al. calculated the reorganization energies of electron transfer between a spherical donor and acceptor and also between a disk-shaped donor and acceptor.[84] Assuming the same volume in the sphere and the disk, the reorganization energy for the sphere model is smaller than that for the disk model, which is quite consistent with our proposal. After the first proposal for the small reorganization energy of fullerenes in 1996, Guldi et al. also demonstrated the small reorganization energy of C_{76} and C_{78} in electron transfer using pulse radiolysis.[85] The reorganization energies of C_{76} and C_{78} have been determined by a charge-shift from the ground states of C_{76} and C_{78} to radical cations of various arenes. The value of λ (0.6 eV in CH_2Cl_2) is much smaller than the typical value (1 eV) in solvents with a similar polarity. The small reorganization energy of fullerenes is quite similar to the situation in the photosynthetic reaction center. In this center efficient, long-lived charge separation is achieved by using multistep electron transfer processes with tuning of reorganization energy to minimize the expenditure of free energies ($-\Delta G_{CS}$) and by forcing the charge recombination well into the Marcus inverted region. In the primary charge separation process from the chlorophyll dimer to the accessory chlorophyll, the reorganization energy (0.2−0.3 eV) is predicted to be small, as mentioned previously. The small value is attributed to the environmental effect of the surrounding protein residues. In contrast, the delocalized π-electron system of fullerenes, with their large size, spherical shape, and high symmetry would make it possible to realize the intrinsic small reorganization energy of fullerenes, which would not be susceptible to changes in surrounding solvents.

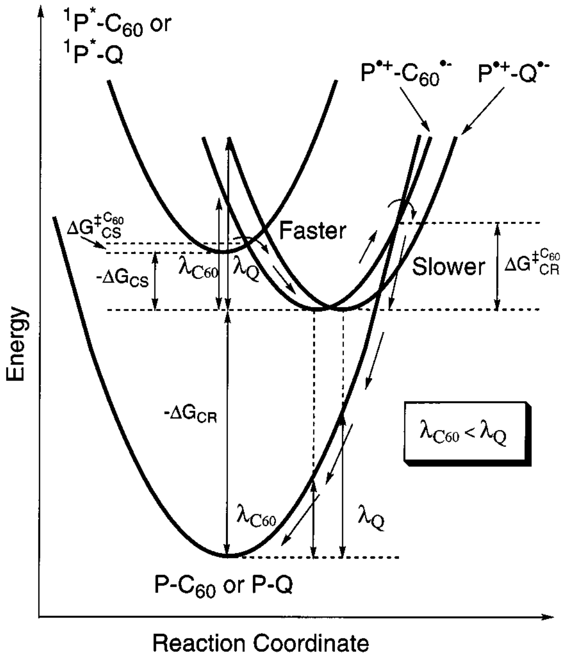

Figure 7. Schematic potential energy surfaces for electron transfer of P−C_{60} **3** and P−Q **7**

Higher fullerenes have a similar three-dimensional size and shape to that of C_{60}.[86] Thus, it is a significant question as to whether the unique property of C_{60} is also maintained in the next most abundant, higher fullerene C_{70}. The shape of C_{70} is like a rugby ball (major axis, 9.8 Å; minor axis, 8.8 Å), in contrast with the soccer ball shape of C_{60} (diameter, 8.8 Å). Irngartinger et al. described the first synthesis and characterization of trimethoxybenzene-linked and anthracene-linked C_{70}.[87] Daub et al. reported the synthesis and preliminary photophysical properties of pyrene-appended C_{60} and C_{70} dyads with the same flexible spacer.[88] The ^{13}C-NMR spectrum of the latter did not allow a reliable assignment of the regiochemistry of the cyclohexane spacer on the C_{70} because of five nonequivalent carbon sites and eight constitutionally distinct C−C bonds on C_{70}. Steady-state fluorescence studies suggested that photoinduced intramolecular energy transfer occurs from the excited singlet state of the pyrene to the C_{60} and C_{70}. However, the details have not been reported. In order to clarify the electron transfer properties in C_{70}, Imahori and Sakata et al. designed compounds **8** and **9** where the same porphyrin unit is attached to C_{70} and C_{60}, using the same rigid spacer (Figures 8 and 9).[89] The regioselective functionalization to C_{60} and C_{70} ensures the well-defined structures of **8** and **9**.[90] Rotational freedom around the methylene spacers in **8** and **9** would not affect the electron transfer rates, a situation that is similar to the previously reported porphyrin−quinones[14] and porphyrin−C_{60} dyads.[18][19] Since the first reduction potentials of C_{60} and C_{70} are reported to be quite similar,[91] the inherent shape and size effect of C_{70} in electron transfer is evaluated accurately by comparing the electron transfer rates of **8** and **9**. Actually, the first reduction potential (−1.10 V vs. Fc/Fc^+) of the C_{70} moiety in **8** is the same as that of the C_{60} moiety in **9**. Absorption spectra of **8** and **9** both in benzene and THF were essentially the linear combinations of the spectra of the corresponding monomer components, indicating no appreciable interactions between the two chromophores in the ground state. The fluorescence spectra of **8** and **9** were strongly quenched compared with those of the porphyrin monomer, showing the rapid quenching of the excited singlet state of the porphyrin (^{1}ZnP*) by the attached fullerenes. We have demonstrated that the direct through-bond electron transfer from the ^{1}ZnP* to the fullerenes is the main pathway in zincporphyrin−C_{60} linked systems where electronic coupling between the two chromophores is weak.[18][21] Considering that (i) there is no apparent interaction between the two moieties in the ground state and (ii) there is no large overlap of the fluorescence from the porphyrin and absorption of the fullerenes, it is concluded that the energy transfer from ^{1}ZnP* to the fullerenes is, at least, not dominant in **8** and **9** in THF and benzene. In other words, photoinduced charge separation from the excited singlet state of the porphyrin to the fullerenes is a major pathway in these solvents. Based on picosecond single-counting fluorescence lifetime measurements, we can estimate the charge separation rates in **8** and **9**. Both in THF and benzene the k_{CS} of **8** is faster than that of **9** by a factor of about 2. The rate acceleration of charge separation is remarkable, considering that the free energy changes for the photoinduced charge separation as well as the electronic couplings between the two moieties are quite similar in **8** and **9**. Although this seems to be explained by the somewhat smaller reorganization energy in C_{70} compared with that in C_{60}, further details will be clarified by carrying out variable temperature studies to separate out the reorganization energy and electronic coupling terms. In conclusion, C_{70} also acts as a good electron acceptor in artificial photosynthetic systems.

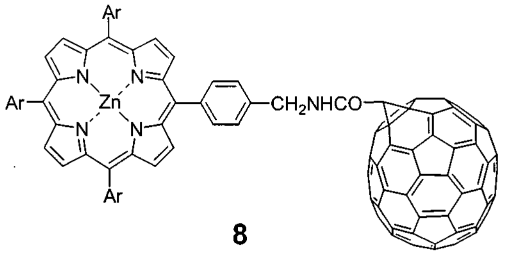

8

Ar=3, 5-(*t*-Bu)$_2$C$_6$H$_3$

Figure 8. Porphyrin−C_{70} dyad **8**

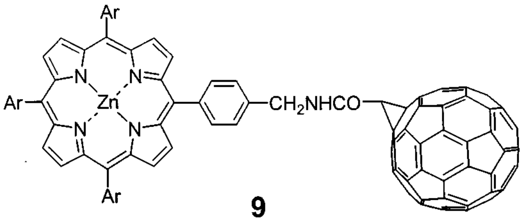

9

Ar=3, 5-(*t*-Bu)$_2$C$_6$H$_3$

Figure 9. Porphyrin−C_{60} dyad **9**

4. Porphyrin−Fullerene Triads

As described in the previous section, the peculiar effect of C_{60} and C_{70} in electron transfer is quite similar to the situation in photosynthetic multistep electron transfer in nature. Therefore, utilization of fullerenes in more elaborate molecular systems such as triads seems to be the next key stage toward the construction of solar energy conversion systems. So far there have been several reports about triads, tetrads, and pentads containing C_{60}.[92−103]

Gust and Moore et al. described the synthesis and photophysical properties of carotenoid (D)−porphyrin (S)−C_{60} (A) triad **10** (Figure 10).[94−96] The energy gradients of each state are designed in the order of $D{-}^1S^*{-}A > D{-}S^{\bullet+}{-}A^{\bullet-} > D^{\bullet+}{-}S{-}A^{\bullet-}$. Accordingly, it was intended that the triad underwent a sequential electron transfer relay, in a similar way to **2**. The characteristic intense absorption band due to the carotenoid cation radical is helpful in the analysis of electron transfer dynamics. In 2-methyltetrahydrofuran, there exists a combination of two pathways to yield $D{-}S^{\bullet+}{-}A^{\bullet-}$; i.e. direct electron transfer from the excited singlet state of the porphyrin to the C_{60} and energy transfer from the excited singlet state of the porphyrin to the C_{60}, followed by successive electron transfer from the porphyrin to the excited singlet state of the C_{60}. A subsequent charge-shift from the carotenoid to the porphyrin cation radical produces $D^{\bullet+}{-}S{-}A^{\bullet-}$ with a low quantum yield of 0.14. The final long-lived charge-separated state decays by charge recombination to yield the carotenoid triplet state with a time constant of 170 ns. Even in a glass state at 77 K, $D^{\bullet+}-S-A^{\bullet-}$ is generated with a quantum yield of 0.10 and recombines to give $^3D^*-S-A$. The authors pointed out two remarkable phenomena, the stepwise electron transfer in a glass state at 77 K and the charge recombination of the final charge-separated state to the triplet state rather than the ground state, two properties that are characteristic of photosynthetic electron transfer in nature. As illustrated in Figure 7, the small reorganization energy of C_{60} decreases the activation barriers for the charge separation as well as the charge-shift, while it increases the activation barriers for the charge recombination. Therefore, the sequential electron transfer would not be greatly affected by a decrease in temperature. In addition, the slower charge recombination of the final charge-separated state to the ground state would enhance the deactivation process to the triplet state.

characteristic bands at 650 nm due to the zincporphyrin cation radical and at 720 nm due to the imide anion radical, were seen. The absorbances at 460 nm, 650 nm, and 720 nm exhibited biphasic decays with time constants of 120 ps and 1.3 ns, whereas an additional rise with a time constant of 30 ps appeared at 650 nm and 720 nm. However, the band at 720 nm due to the imide anion radical decays much faster (120 ps) than the $S^{\bullet+}$, with the sole remaining broad absorption being due to the $S^{\bullet+}$, which decays with a time constant of 1.3 ns. Although it was difficult to detect the C_{60} anion radical under the experimental conditions, these results clearly show the photoinduced two-step electron transfer in **11**: the initial formation of $S^{\bullet+}-A_1^{\bullet-}-A_2$, followed by the charge-shift to produce $S^{\bullet+}-A_1-A_2^{\bullet-}$ with a moderate quantum yield of 0.46 (Figure 13). It is remarkable that the charge-shift from the imide anion radical to the C_{60} is able to compete with the reverse electron transfer to the ground state, despite the small difference (0.08 V) in electron-accepting abilities between the imide and the C_{60} moieties. It should be noted here that the first-step electron transfer in **11** is faster by 50% compared with that of the corresponding porphyrin−imide dyad. Although this may be explained by the acceleration effect of C_{60} in electron transfer *through the bond* or *through the space*, further details must await photodynamical experiments on related compounds. In more polar solvents, like THF, the excitation of **11** leads to the formation of $S^{\bullet+}-A_1^{\bullet-}-A_2$ within 20 ps, but the charge recombination rate is much faster than the charge separation rate, resulting in the $S^{\bullet+}-A_1-A_2^{\bullet-}$ state not being detected.

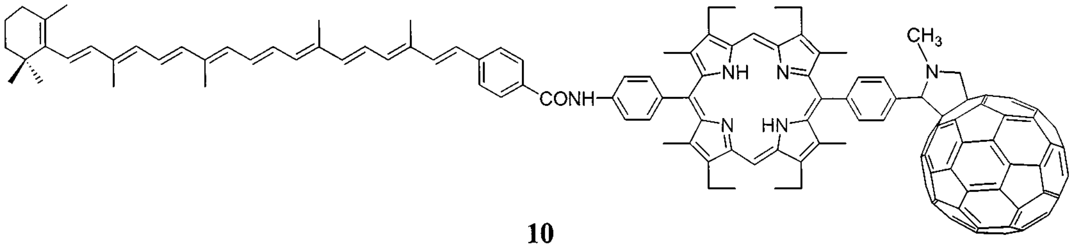

10

Figure 10. Carotenoid−porphyrin−C_{60} triad **10** mimicking photoinduced multistep electron transfer in photosynthesis

Imahori and Sakata et al. have presented the synthesis and photophysical properties of porphyrin (S)−pyromellitimide (A_1)−C_{60} (A_2) triad **11** (Figure 11).[97] Considering that the energy gradient of **11** is quite similar to that of **1**, the triad **11** is expected to exhibit the same sequential electron transfer as that in photosynthetic electron transfer. Besides, the linear conformation as well as the characteristic intense band due to the imide anion radical ($Im^{\bullet-}$) make it possible to analyze the photodynamic properties accurately.

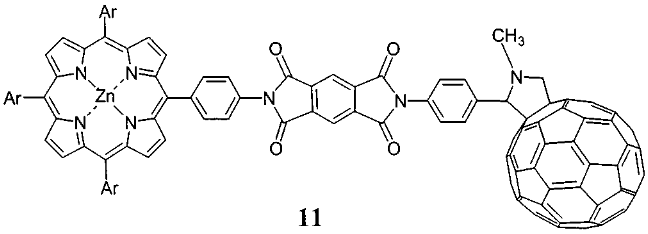

11

Ar=3, 5-(*t*-Bu)$_2$C$_6$H$_3$

Figure 11. Porphyrin−pyromellitimide−C_{60} triad **11** mimicking photoinduced multistep electron transfer in photosynthesis

The absorption spectra and redox potentials of **11** are roughly explained by the sum of the three chromophores, indicating that there is no significant interaction between the three chromophores in the ground state. The time-resolved transient absorption spectra of **11** were taken in dioxane and are shown in Figure 12. Immediately after the excitation of **11** the bleaching of the ground-state porphyrin absorption of the Q-bands, an intense band at 470 nm, and

Imahori and Sakata et al. described the synthesis and photophysical properties of diporphyrin−fullerene triad **12**, which is shown in Figure 14.[103] It is well-known that efficient singlet-singlet energy transfer occurs from the excited singlet state of a zincporphyrin to a free-base porphyrin in typical diporphyrin dyads.[5] It has also been reported that a charge-separated state or an exciplex is generated in free-base porphyrin−C_{60} dyads when the free-base porphyrin is excited in polar solvents. Thus, the diporphyrin attached to C_{60} is expected to display sequential energy transfer and charge separation processes that mimic both the energy transfer process in the light-harvesting complex and the subsequent photoinduced charge separation process in the reaction center.

The synthesis of **12** includes selective insertion of a zinc atom into the diporphyrin and its protection from demetallation. Therefore, neutral or basic experimental conditions

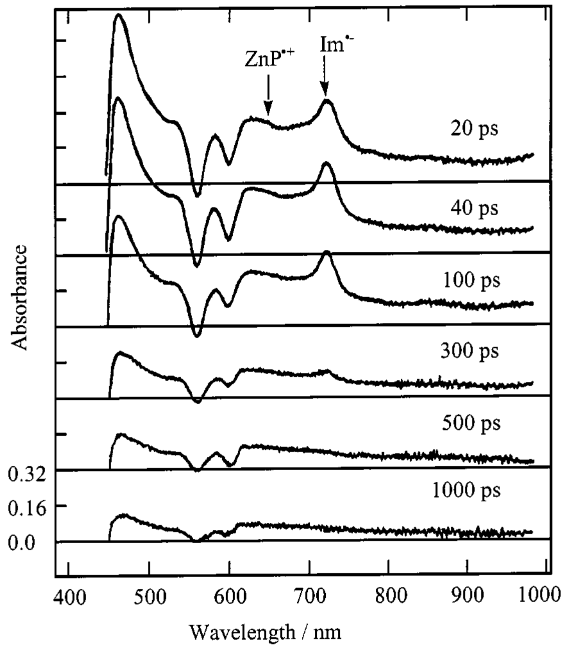

Figure 12. Picosecond time-resolved transient absorption spectra of **11** in dioxane excited at 590 nm; the delay times between excitation and measurement are indicated on the right

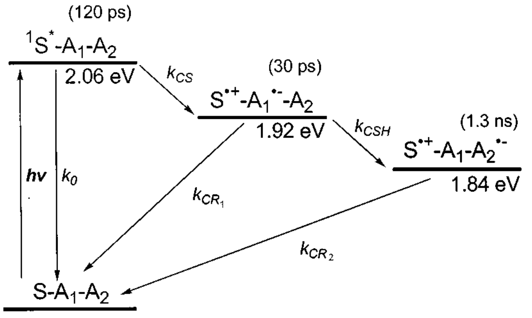

Figure 13. Reaction scheme and energy diagram for **11** in dioxane. Numbers in parentheses indicate the lifetimes of the each states. The rate constants of each processes are k_0 = 5.0·10^8 s^{-1}, k_{CS} = 7.8·10^9 s^{-1}, k_{CR1} = 1.7·10^{10} s^{-1}, k_{CSH} = 1.6·10^{10} s^{-1}, and k_{CR2} = 7.7·10^8 s^{-1}.

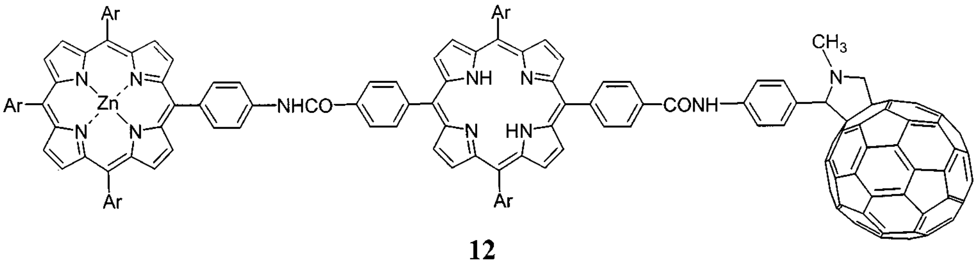

12

Ar=3, 5-(t-Bu)$_2$C$_6$H$_3$

Figure 14. Diporphyrin−C$_{60}$ triad **12** mimicking both energy transfer in the antenna complex and charge separation in the reaction center

are essential for the transformation. Absorption due to the two porphyrin chromophores is much stronger than that of the C$_{60}$, implying that the diporphyrin moieties are a major light-collector in **12**. Fluorescence lifetimes of **12** in THF were investigated using a picosecond single photon counting technique with both excitation of the porphyrins and monitoring at 655 and 720 nm, the region where the emission is mainly due to both the porphyrins and the free-base porphyrin, respectively. The fluorescence decay of **12** at 655 nm was analyzed by two exponential decays with time constants of 43 ps (A = 0.20) and 1.6 ns (A = 0.80). In contrast, the emission at 720 nm was fitted by a rise with a time constant of 43 ps and a decay with a time constant of 1.7 ns (A = 1.00). The matching of the time constants between the decay and the rise in **12** strongly supports the efficient energy transfer (2.3·10^{10} s^{-1}) from the excited singlet state of the zincporphyrin to the free-base porphyrin in THF. The shorter time constant (τ = 1.7 ns) of **12**, due to the free-base porphyrin, compared with that of the free-base porphyrin monomer (9.9 ns), indicates the photoinduced electron transfer or charge-transfer from the excited singlet state of the free-base porphyrin to C$_{60}$. These results suggest that initial photoinduced energy transfer from the excited singlet state of the zincporphyrin to the free-base porphyrin and subsequent charge separation from the excited singlet state of the free-base porphyrin to C$_{60}$ take place in **12**.

These examples show clearly that C$_{60}$ is a suitable component to build up photoinitiated multistep electron transfer systems.

5. Application of Fullerenes as Photovoltaic Cells

In the previous sections, fullerenes have been shown to be excellent building blocks in artificial photosynthetic models. In other words, "photosynthesis" could be realized in a fullerene-containing single molecule system where an energetic, long-lived charge-separated state is generated with a high quantum yield. However, to convert the charge-separated state into photocurrents or chemical energy for practical use, a unidirectional molecular assembly of the single molecules is required at the nano-scale level. Although Langmuir−Blodgett and lipid bilayer membranes have been used for the organization of the molecules, these attempts did not give fruitful results (the overall quantum yield = 1−10%) due to the instability of, and presence of defects in, the artificial membranes.[104−111] Self-assembled monolayers have recently attracted considerable attention as a new methodology for molecular assembly.[112] They enable the molecules of interest to be bound chemically onto surfaces such as metals, semiconductors, and insulators in a highly organized manner. Thus, they make it possible to arrange functional molecules unidirectionally at the molecular level on substrates when substituents that will self-assemble on the substrates are attached to a terminal position in the molecules. A wide variety of examples have been reported to date involving functional molecules such as ferrocenes, azobenzenes, fullerenes, porphyrins, cyclodextrins, proteins, and others.

The self-assembled monolayers technique has been applied to porphyrin-linked C_{60} compound **13** to mimic supramolecular photoinduced charge-separation events in photosynthesis as shown in Figure 15.[113–115] It is known that porphyrins bearing a thiol group are susceptible to oxidation by oxygen and/or light. In contrast, sulfides are relatively stable compared with thiols and disulfides. Therefore, as the first stage we have chosen a simple methylthio group at one end of a porphyrin ring, while the opposite end has a C_{60} moiety. Structures of the self-assembled monolayers formed on gold electrodes were studied by spectroscopic methods including X-ray photoelectron spectroscopy, ultraviolet-visible spectroscopic ellipsometry, ultraviolet-visible absorption spectroscopy, and Fourier transform infrared spectroscopy as well as electrochemical studies. It is concluded from the experiments that the self-assembled monolayers have loosely packed structures; the porphyrin–C_{60} molecules are tilted and nearly parallel with the gold surface. Photoelectrochemical measurements were carried out in an argon-saturated Na_2SO_4 solution, containing methylviologen as an electron carrier, using the modified gold electrode as a working electrode and a platinum counter electrode. Short-circuit cathodic photocurrent with a level of sub-μA/cm^2 was observed for the photoelectrochemical cell under illumination with ca. 4 mW/cm^2; the quantum yield is ca. 0.5%. The intensity of the photocurrent in the free-base porphyrin–C_{60} system is five times larger compared with that in the corresponding free-base porphyrin monomer system, indicating that C_{60} is an effective mediator in multistep electron transfer processes. The intensity of the photocurrent in the free-base porphyrin–C_{60} cell is about one order of magnitude larger than that in the zincporphyrin–C_{60} cell. The photocurrent generation in self-assembled monolayers of porphyrin–C_{60} systems can be explained by two different electron transport mechanisms: an ion pair mechanism for the zincporphyrin–C_{60} cell and an exciplex mechanism for the free-base porphyrin–C_{60} cell. The shorter lifetime in the charge-separated state of the former leads to a poor generation of the photocurrent, while the longer lifetime in the exciplex of the latter results in a pronounced increase in the photocurrent.

The low quantum yields of the photocurrent can be ascribed to the loosely packed monolayers of the porphyrin–fullerene conjugates. In order to obtain information about the relationship between molecular structure and the structure of monolayers, disulfides **14** (n = 1, 3, 5, 7, 10), with a series of alkyl spacers containing porphyrins at both ends, were prepared as a simple model (Figure 16).[116][117]

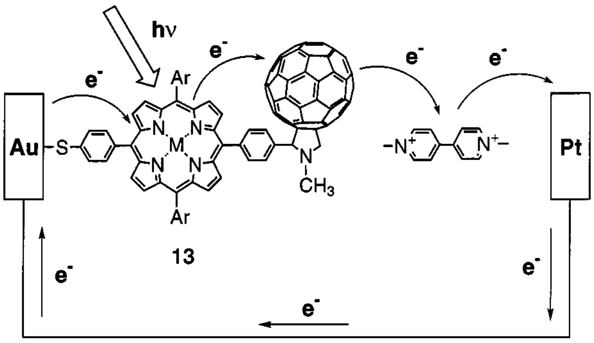

13

Ar=3, 5-(t-Bu)$_2$C$_6$H$_3$

Figure 15. Photoinduced multistep electron transfer at gold electrodes modified with self-assembled monolayers of porphyrin–C_{60} dyads **13** (M = H_2, Zn)

The spectroscopic studies showed that the self-assembled monolayers form a highly ordered structure on the gold electrode when the porphyrins possess methylene spacers of suitable length (n = 7). Photoelectrochemical studies, using modified gold and platinum electrodes, were carried out in the presence of methylviologen as an electron carrier. A cathodic photoelectrochemical response was detected when the light was switched on and off. The quantum yields were up to 0.1% (n = 10). The short-circuit photocurrents in the two electrode system decreased dramatically with a decrease in the spacer length. This clearly shows that two competitive deactivation pathways exist for the excited porphyrin, i.e. quenching by the gold electrode through energy transfer and by electron carriers through electron transfer, as illustrated in Figure 16.

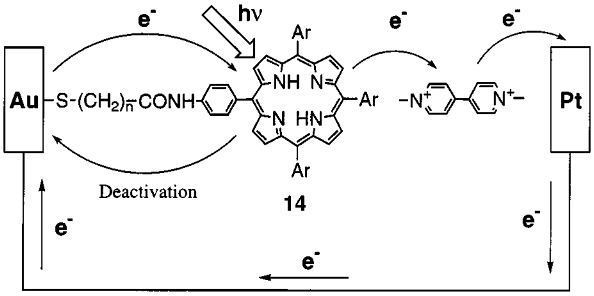

14

Ar=3, 5-(t-Bu)$_2$C$_6$H$_3$

Figure 16. Photoinduced multistep electron transfer at gold electrodes modified with self-assembled monolayers of porphyrins **14** with different spacer lengths (n = 1, 3, 5, 7, 10)

A highly ordered monolayer containing C_{60} is also formed on a gold electrode when C_{60}-attached polyalkanethiol **15** is self-assembled on the gold electrode (Figure 17).[118][119] A photoelectrochemical experiment was carried out using the C_{60}-modified gold electrode as a working electrode, a platinum wire as a counter electrode, and an Ag/AgCl electrode as a reference. A stable anodic photocurrent was observed in the presence of an electron sacrificer when the modified gold electrode was illuminated with a monochromic light. This suggests the generation of a vectorial electron flow from the electron sacrificer to the gold electrode via the excited states of the C_{60}. The quantum yield (9.8%) is comparable to similar C_{60} cells using lipid bilayers and Langmuir−Blodgett membranes.[120][121] The highly ordered monolayer, as well as the peculiar effect of the C_{60} in electron transfer, would greatly improve the performance of photoelectrochemical cells of this type.

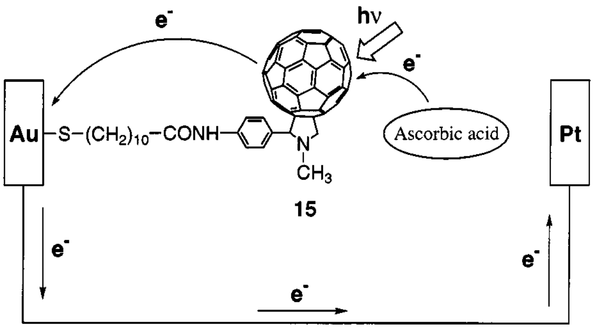

Ar=3, 5-(*t*-Bu)$_2$C$_6$H$_3$

Figure 17. Photoinduced multistep electron transfer at a gold electrode modified with a self-assembled monolayer of C_{60} **15**

Imahori and Sakata et al. have extended these systems and developed for the first time an artificial photosynthetic cell with a gold electrode modified with a self-assembled monolayer of fullerene-containing triad.[122][123] The alkanethiol-attached triad **16** involves a linear array of ferrocene (D), porphyrin (S), and C_{60} (A), as shown in Figure 18. The energy gradients of each state in the triad are in the order $D-{}^1S^*-A > D-S^{\bullet+}-A^{\bullet-} > D^{\bullet+}-S-A^{\bullet-}$. Therefore, it will display a sequential electron transfer, as observed in **2** and **10**. In addition, utilization of C_{60} as an acceptor in the triad will allow us to realize artificial multistep electron transfer processes with a longer lifetime and a higher quantum efficiency within a molecule. The tethered polyalkanethiol makes it possible to arrange the triad **16** unidirectionally on a gold electrode, leading to the formation of a uniform self-assembled monolayer with a thickness of ca. 50 Å. Accordingly, a combination of the triad involving C_{60} and the self-assembled monolayer seems to be a potential strategy to build up an efficient light-energy conversion system.

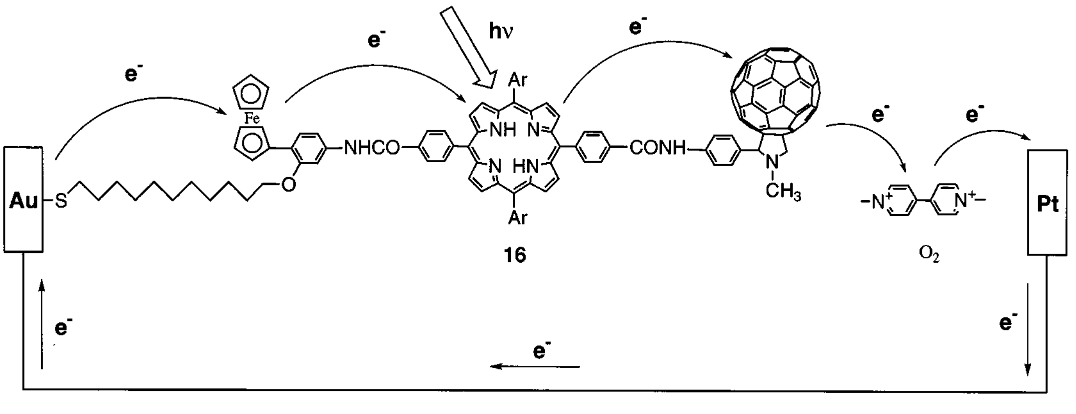

Ar=3, 5-(*t*-Bu)$_2$C$_6$H$_3$

Figure 18. Photoinduced multistep electron transfer at a gold electrode modified with a self-assembled monolayer of ferrocene−porphyrin−C_{60} triad **16**

Steady-state fluorescence studies in solutions suggest that the quenching of the excited singlet porphyrin by the attached C_{60} is a dominant deactivation pathway in **16**. A cyclic voltammetric experiment using the modified gold electrode was performed to estimate the surface coverage. An adsorbed amount of **16** on the gold electrode was calculated to be $1.9 \cdot 10^{-10}$ mol cm^{-2} (= 86 Å^2 molecule^{-1}), which is comparable to those in the well-ordered self-assembled monolayers of porphyrins and fullerenes on gold electrodes.[117−119] The results indicate that the triad molecules are well-packed with almost perpendicular orientation on the gold surface.

Photoelectrochemical experiments using triad-modified gold, a platinum wire, and Ag/AgCl electrodes were carried out in the presence of electron carriers such as oxygen and/or methylviologen. A cathodic photocurrent was observed during the irradiation of the modified gold electrode. The net intensity of the photocurrent in the present system is larger by two orders of magnitude than that in the porphyrin−polyalkanethiol systems,[117] which implies that the C_{60} and the ferrocene moieties are responsible for the higher efficiency. An increase in the cathodic photocurrent with an increase of the negative bias to the gold electrode, demonstrates the direction of the electron flow from the gold electrode to the counter electrode through the electrolyte. When the potential was applied more negative at +500 mV, the intensity of the photocurrent dramatically increased. Based on the matching of the value with the oxidation potential of the ferrocene [+510 mV (Fc/Fc$^+$)], it can be concluded that the efficiency is controlled by the electron transfer rate between the gold electrode and the ferrocene. The action spectrum of the cell is in good agreement with the absorption spectrum of **16** on the gold electrode, indicating clearly that the porphyrin is a major photoactive species for the photocurrent generation. Under the optimal conditions using an oxygen-saturated solution in the presence of methylviologen, the quantum yield was found to be 25%, which is more than two times larger than the highest value (11%) in the previously reported photosynthetic electron transfer across artificial membranes and at monolayer-modified metal electrodes.[104−125]

The photocurrent generation may be explained as follows. Photoinduced electron transfer or partial charge-transfer (formation of an exciplex) takes place from the excited singlet state of the porphyrin [−750 mV ($^1P^*/P^{\bullet +}$)] to the C_{60} [−620 mV ($C_{60}/C_{60}^{\bullet -}$)].[114][115] The resulting $C_{60}^{\bullet -}$ gives an electron to diffusing electron carriers such as oxygen [−480 mV ($O_2/O_2^{\bullet -}$)] and/or methylviologen [−620 mV ($MV^{2+}/MV^{\bullet +}$)], which eventually transfer an electron to the counter electrode. On the other hand, an electron migration occurs from the gold electrode to the porphyrin cation radical via the ferrocene, thereby recovering the initial state. Overall, a cathodic electron flow occurs from the gold electrode to the counter electrode through the monolayer. In order to obtain efficient photoinduced multistep electron transfer at the gold electrode, the initial photoinduced electron transfer from the excited singlet state of the porphyrin to the first acceptor must compete with the deactivation due to the gold electrode, as we demonstrated in the self-assembled monolayers of porphyrins.[117] In addition, the charge shift from the first acceptor to the diffusing electron carriers or from the ferrocene to the porphyrin cation radical must be much faster than the charge recombination to the ground state. Utilization of C_{60} with its small reorganization energy may fully satisfy the requirements and improve the quantum yield greatly.

6. Conclusion and Outlook

Fullerenes have been found to be excellent acceptors by investigating photoinduced intramolecular electron transfer in porphyrin-linked C_{60} and C_{70} molecules using picosecond time-resolved spectroscopic methods. The most intriguing characteristics of C_{60} in electron transfer are the acceleration of photoinduced charge separation and the slowing down of charge recombination. A comparison between the photoinduced charge separation rates in porphyrin−C_{60} and porphyrin−C_{70} dyads revealed that the unique properties of C_{60} in electron transfer are also maintained in C_{70}. These results indicate that the electron transfer properties of fullerenes are related to the three-dimensional delocalized π systems that have large size, spherical strained shape, and high symmetry. Porphyrin−imide−C_{60} triad displays a stepwise electron transfer relay that mimics the primary charge separation in the photosynthetic reaction center. It should be noted that the C_{60} moiety in the triad accelerates photoinduced charge separation *directly* or *indirectly*. Diporphyrin−C_{60} triad mimics photosynthetic energy transfer in the antenna complex as well as electron transfer in the reaction center complex. These results clearly show that fullerenes are good building blocks for the construction of artificial photosynthetic multicomponent systems. The more elaborate fullerene-containing systems such as tetrads and pentads will be the next synthetic target as artificial photosynthetic models that can demonstrate multistep electron transfer relay with a long-lived charge-separated state in a high quantum yield.

The availability of fullerenes in macroscopic quantities has made it possible to develop the photoinduced electron transfer chemistry of fullerenes. The fact that C_{60} and C_{70} exhibit novel properties in electron transfer stimulates development of new electron transfer chemistry where the three-dimensional structures of donors and acceptors are important. Thus, higher fullerenes, heterofullerenes, carbon nanotubes, and clusters as well as well-designed “three-dimensional” molecules also seem to be good candidates as electron donors, electron acceptors, and electron accumulators. Control of the reorganization energies in electron transfer will be accomplished using these synthetic molecules.

We have demonstrated that the peculiar effect of fullerenes in electron transfer can be explained by the small reorganization energy of fullerenes in electron transfer. We propose a novel strategy of engineering artificial photosynthetic charge-separating systems by choosing suitable redox pairs and adjusting electronic coupling, free energy change, and reorganization energy. The strategy involves utilization of photosynthetic multistep electron transfer and fullerenes with small reorganization energies. It allows us to construct artificial photosynthetic systems with efficient and long-lived charge separation, where the number of electron transfer steps and energy loss are minimized. Applying this novel strategy to the construction of solar energy conversion systems has been carried out in self-assembled monolayers on electrodes. These systems include porphyrins, fullerenes, and porphyrin-linked C_{60} dyads and triads. The highly ordered monolayers are formed on gold electrodes when the functional molecules are attached to polyalkanethiols. The modified gold electrodes have been used to construct the photoelectrochemical cells that mimic photosynthetic multistep electron transfer at the membrane. The quantum yield of the ferrocene−porphyrin−C_{60} triad cell is 25%, which is the highest value among the previously reported artificial photosynthetic electron transfer in the artificial membranes and at the metal electrodes modified with monolayers. The results clearly show that our strategy is very effective for constructing artificial photosynthetic materials that are significantly different from conventional inorganic solar cells. Further improvements in the efficiency will be possible by modifying the chromophores, changing the nature of the spacer, and selecting suitable substrates as electrodes.

Our approach using fullerenes as acceptors, as well as molecular technologies on substrates using self-assembled monolayers, will open the door to develop molecule-based artificial photosynthetic materials with high efficiencies. Such molecular devices will stimulate many fields, such as chemistry, physics, and biology to develop new principles and concepts in nano-scale science and technology toward the next century

Acknowledgments

This work was supported by Grant-in-Aids for COE Research and Scientific Research on Priority Area of Electrochemistry of Ordered Interfaces and Creation of Delocalized Electronic Systems from Ministry of Education, Science, Sports and Culture, Japan. Y. S. thanks the Mitsubishi Foundation for financial support. The authors are indebted to their colleagues and co-workers, particularly Professor Tadashi Okada at Osaka University and Professor Iwao Yamazaki at Hokkaido University, for much of the work that is contained herein.

---

[1] J. Deisenhofer, J. R. Norris (Eds.), *The Photosynthetic Reaction Center*, Academic Press, San Diego, **1993**.

[2] J. S. Connolly, J. R. Bolton in: *Photoinduced Electron Transfer, Part D* (Eds.: M. A. Fox, M. Chanon), Elsevier, Amsterdam, **1988**, p. 303.

[3] M. R. Wasielewski in: *Photoinduced Electron Transfer, Part A* (Eds.: M. A. Fox, M. Chanon), Elsevier, Amsterdam, **1988**, p. 161.

[4] M. R. Wasielewski, *Chem. Rev.* **1992**, *92*, 435.

[5] D. Gust, T. A. Moore, A. L. Moore, *Acc. Chem. Res.* **1993**, *26*, 198.

[6] K. Maruyama, A. Osuka, N. Mataga, *Pure Appl. Chem.* **1994**, *66*, 867.

[7] H. Kurreck, M. Huber, *Angew. Chem. Int. Ed. Engl.* **1995**, *34*, 849.

[8] M. Migita, T. Okada, N. Mataga, S. Nishitani, N. Kurata, Y. Sakata, S. Misumi, *Chem. Phys. Lett.* **1981**, *84*, 263.

[9] S. Nishitani, N. Kurata, N. Nishimizu, Y. Sakata, S. Misumi, T. Okada, N. Mataga, 6th Symposium on structural organic chemistry (Kyoto), **1982**, B2−20; S. Nishitani, N. Kurata, Y. Sakata, S. Misumi, A. Karen, T. Okada, N. Mataga, *J. Am. Chem. Soc.* **1983**, *105*, 7771.

[10] T. A. Moore, D. Gust, P. Mathis, J.-C. Mialocq, C. Chachaty, R. V. Bensasson, E. J. Land, D. Doizi, P. A. Liddell, W. R. Lehman, G. A. Nemeth, A. L. Moore, *Nature* **1984**, *307*, 630.

[11] D. Gust, T. A. Moore, A. L. Moore, A. N. Macpherson, A. Lopez, J. M. DeGraziano, I. Gouni, E. Bittersmann, G. R. Seely, F. Gao, R. A. Nieman, X. C. Ma, L. J. Demanche, S.-C. Hung, D. K. Luttrull, S.-J. Lee, P. K. Kerrigan, *J. Am. Chem. Soc.* **1993**, *115*, 11141.

[12] R. A. Marcus, *J. Chem. Phys.* **1956**, *24*, 966; R. A. Marcus, *J. Chem. Phys.* **1965**, *43*, 679; R. A. Marcus, N. Sutin, *Biochim. Biophys. Acta* **1985**, *811*, 265; R. A. Marcus, *Angew. Chem. Int. Ed. Engl.* **1993**, *32*, 1111.

[13] C. C. Moser, J. M. Keske, K. Warncke, R. S. Farid, P. L. Dutton, in: *The Photosynthetic Reaction Center, Vol. II* (Eds.: J. Deisenhofer, J. R. Norris), Academic Press, San Diego, **1993**, p.1.

[14] T. Asahi, M. Ohkohchi, R. Matsusaka, N. Mataga, R. P. Zhang, A. Osuka, K. Maruyama, *J. Am. Chem. Soc.* **1993**, *115*, 5665.

[15] J. M. DeGraziano, P. A. Liddell, L. Leggett, A. L. Moore, T. A. Moore, D. Gust, *J. Phys. Chem.* **1994**, *98*, 1758.

[16] P. A. Liddell, J. P. Sumida, A. N. Macpherson, L. Noss, G. R. Seely, K. N. Clark, A. L. Moore, T. A. Moore, D. Gust, *Photochem. Photobiol.* **1994**, *60*, 537.

[17] H. Imahori, Y. Sakata, 7th Symposium on C_{60} (Nagoya), **1994**, 200; K. Hagiwara, S. Taniguchi, M. Hasegawa, T. Okada, H. Imahori, Y. Sakata, Symposium on Photochemistry (Osaka), **1994**, IA113; H. Imahori, K. Hagiwara, T. Akiyama, S. Taniguchi, T. Okada, Y. Sakata, *Chem. Lett.* **1995**, 265; H. Imahori, Y. Sakata, *Mem. Inst. Sci. Ind. Res., Osaka Univ.* **1995**, *52*, 69.

[18] H. Imahori, K. Hagiwara, M. Aoki, T. Akiyama, S. Taniguchi, T. Okada, M. Shirakawa, Y. Sakata, *J. Am. Chem. Soc.* **1996**, *118*, 11771; H. Imahori, M. Aoki, T. Akiyama, Y. Sakata, K. Hagiwara, T. Okada, *Proc. of the Symp. on Recent Advances in the Chemistry and Physics of Fullerenes and Related Materials, Vol. 3* (Eds.: K. M. Kadish, R. S. Runoff), The Electrochemical Society, Pennington, NJ, **1996**, p. 332.

[19] H. Imahori, K. Hagiwara, T. Akiyama, M. Aoki, S. Taniguchi, T. Okada, M. Shirakawa, Y. Sakata, *Chem. Phys. Lett.* **1996**, *263*, 545.

[20] A. W. Jensen, S. R. Wilson, D. I. Schuster, *Bioorg. Med. Chem.* **1996**, *4*, 767.

[21] H. Imahori, Y. Sakata, *Adv. Mater.* **1997**, *9*, 537.

[22] D. Gust, T. A. Moore, A. L. Moore, *Res. Chem. Intermed.* **1997**, *23*, 621.

[23] M. Prato, M. Maggini, *Acc. Chem. Res.* **1998**, *31*, 519.

[24] A. L. Balch, M. M. Olmstead, *Chem. Rev.* **1998**, *98*, 2123.

[25] N. Martín, L. Sánchez, B. Illescas, I. Pérez, *Chem. Rev.* **1998**, 98, 2527.

[26] S. I. Khan, A. M. Oliver, M. N. Paddon-Row, Y. Rubin, *J. Am. Chem. Soc.* **1993**, *115*, 4919.

[27] M. Maggini, G. Scorrano, M. Prato, *J. Am. Chem. Soc.* **1993**, *115*, 9798.

[28] T. Tago, T. Minowa, Y. Okada, J. Nishimura, *Tetrahedron Lett.* **1993**, *34*, 8461.

[29] F. Diederich, U. Jonas, V. Gramlich, A. Herrmann, H. Ringsdorf, C. Thilgen, *Helv. Chim. Acta* **1993**, *76*, 2445.

[30] P. Belik, A. Gügel, A. Kraus, J. Spickermann, V. Enkelmann, G. Frank, K. Müllen, *Adv. Mater.* **1993**, *5*, 854.

[31] M. Maggini, A. Karlsson, G. Scorrano, G, Sandonà, G. Farnia, M. Parto, *J. Chem. Soc., Chem. Commun.* **1994**, 589.

[32] A. Gügel, A. Kraus, J. Spickermann, P. Belik, K. Müllen, *Angew. Chem. Int. Ed. Engl.* **1994**, *33*, 559.

[33] M. Rasinkangas, T. T. Pakkanen, T. A. Pakkanen, *J. Organomet. Chem.* **1994**, *476*, C6.

[34] R. M. Williams, J. M. Zwier, J. W. Verhoeven, *J. Am. Chem. Soc.* **1995**, *117*, 4093.

[35] T. G. Linssen, K. Dürr, M. Hanack, A. Hirsch, *J. Chem. Soc., Chem. Commun.* **1995**, 103.

[36] H. Imahori, S. Cardoso, D. Tatman, S. Lin, L. Noss, G. R. Seely, L. Sereno, J. C. de Silber, T. A. Moore, A. L. Moore, D. Gust, *Photochem. Photobiol.* **1995**, *62*, 1009.

[37] T. Drovetskaya, C. A. Reed, P. D. W. Boyd, *Tetrahedron Lett.* **1995**, *36*, 7971.

[38] M. Maggini, A. Donò, G. Scorrano, M. Prato, *J. Chem. Soc., Chem. Commun.* **1995**, 845.

[39] Y. Nakamura, T. Minowa, S. Tobita, H. Shizuka, J. Nishimura, *J. Chem. Soc., Perkin Trans. 2* **1995**, 2351.

[40] S. Sariciftci, F. Wudl, A. J. Heeger, M. Maggini, G. Scorrano, M. Prato, J. Bourassa, P. C. Ford, *Chem. Phys. Lett.* **1995**, *247*, 510.

[41] D. Armspach, E. C. Constable, F. Diederich, C. E. Housecroft, J.-F. Nierengarten, *J. Chem. Soc., Chem. Commun.* **1996**, 2009.

[42] D. Kuciauskas, S. Lin, G. R. Seely, A. L. Moore, T. A. Moore, D. Gust, T. Drovetskaya, C. A. Reed, P. D. W. Boyd, *J. Phys. Chem.* **1996**, *100*, 15926.

[43] H. Imahori, Y. Sakata, *Chem. Lett.* **1996**, 199.

[44] M. G. Ranasinghe, A. M. Oliver, D. F. Rothenfluh, A. Salek, M. N. Paddon-Row, *Tetrahedron Lett.* **1996**, *37*, 4797.

[45] J. M. Lawson, A. M. Oliver, D. F. Rothenfluh, Y.-Z. An, G. A. Ellis, M. G. Ranasinghe, S. I. Khan, A. G. Franz, P. S. Ganapathi, M. J. Shephard, M. N. Paddon-Row, Y. Rubin, *J. Org. Chem.* **1996**, *61*, 5032.

[46] R. M. Williams, M. Koeberg, J. M. Lawson, Y.-Z. An, Y. Rubin, M. N. Paddon-Row, J. W. Verhoeven, *J. Org. Chem.* **1996**, *61*, 5055.

[47] Y. Nakamura, T. Minowa, Y. Hayashida, S. Tobita, H. Shizuka, J. Nishimura, *J. Chem. Soc., Faraday Trans.* **1996**, *92*, 377.

[48] Y. Nakamura, M. Taki, T. Minowa, J. Nishimura, *J. Synth. Org. Chem. Jpn.* **1996**, *54*, 574.

[49] N. Martín, L. Sánchez, C. Seoane, R. Andreu, J. Garín, J. Orduna, *Tetrahedron Lett.* **1996**, *37*, 5979.

[50] T. D. M. Bell, T. A. Smith, K. P. Ghiggino, M. G. Ranasinghe, M. J. Shephard, M. N. Paddon-Row, *Chem. Phys. Lett.* **1997**, *268*, 223.

[51] Y. Sakata, H. Imahori, H. Tsue, S. Higashida, T. Akiyama, E. Yoshizawa, M. Aoki, K. Yamada, K. Hagiwara, S. Taniguchi, T. Okada, *Pure Appl. Chem.* **1997**, *69*, 1951.

[52] A. L. Moore, T. A. Moore, D. Gust, J. J. Silber, L. Sereno, F. Fungo, L. Otero, G. Steinberg-Yfrach, P. A. Liddell, S.-C. Hung, H. Imahori, S. Cardoso, D. Tatman, A. N. Macpherson, *Pure Appl. Chem.* **1997**, *69*, 2111.

[53] Y. Sun, T. Drovetskaya, R. D. Bolskar, R. Bau, P. D. W. Boyd, C. A. Reed, *J. Org. Chem.* **1997**, *62*, 3642.

[54] P. S. Baran, R. R. Monaco, A. U. Khan, D. I. Schuster, S. R. Wilson, *J. Am. Chem. Soc.* **1997**, *119*, 8363.

[55] I. G. Safonov, P. S. Baran, D. I. Schuster, *Tetrahedron Lett.* **1997**, *38*, 8133.

[56] K. Dürr, S. Fiedler, T. Linßen, A. Hirsch, M. Hanack, *Chem. Ber.* **1997**, 130, 1375.

[57] D. M. Guldi, M. Maggini, G. Scorrano, M. Prato, *J. Am. Chem. Soc.* **1997**, *119*, 974.

[58] C. Boulle, J. M. Rabreau, P. Hudhomme, M. Cariou, M. Jubault, A. Gorgues, J. Orduna, J. Garín, *Tetrahedron Lett.* **1997**, *38*, 3909.

[59] G. Torres-Garcia, H. Luftmann, C. Wolff, J. Mattay, *J. Org. Chem.* **1997**, *62*, 2752.
[60] N. Martín, I. Pérez, L. Sánchez, C. Seoane, *J. Org. Chem.* **1997**, *62*, 5690.
[61] J. Llacay, J. Veciana, J. Vidal-Gancedo, J. L. Bourdelande, R. González-Moreno, C. Rovira, *J. Org. Chem.* **1998**, *63*, 5201.
[62] E. Dietel, A. Hirsch, J. Zhou, A. Rieker, *J. Chem. Soc., Perkin Trans. 2* **1998**, 1357.
[63] H. Maruyama, M. Fujiwara, K. Tanaka, *Chem. Lett.* **1998**, 805.
[64] K. G. Thomas, V. Biju, M. V. George, D. M. Guldi, P. V. Kamat, *J. Phys. Chem. A* **1998**, *102*, 5341.
[65] M. Diekers, A. Hirsch, S. Pyo, J. Rivera, L. Echegoyen, *Eur. J. Org. Chem.* **1998**, 1111.
[66] T. Gareis, O. Köthe, J. Daub, *Eur. J. Org. Chem.* **1998**, 1549.
[67] Y.-P. Sun, B. Ma, C. E. Bunker, *J. Phys. Chem. A* **1998**, *102*, 7580.
[68] E. Dietel, A. Hirsch, E. Eichhorn, A. Rieker, S. Hackbarth, B. Röder, *Chem. Commun.* **1998**, 1981.
[69] J.-P. Bourgeois, F. Diederich, L. Echegoyen, J.-F. Nierengarten, *Helv. Chim. Acta* **1998**, *81*, 1835.
[70] D. M. Guldi, G. Torres-Garcia, J. Mattay, *J. Phys. Chem. A* **1998**, *102*, 9679.
[71] A. C. Tomé, R. F. Enes, J. P. C. Tomé, J. Rocha, M. G. P. M. S. Neves, J. A. S. Cavaleiro, J. Elguero, *Tetrahedron* **1998**, *54*, 11141.
[72] F. Effenberger, G. Grube, *Synthesis* **1998**, 1372.
[73] M. Maggini, D. M. Guldi, S. Mondini, G. Scorrano, F. Paolucci, P. Ceroni, S. Roffia, *Chem. Eur. J.* **1998**, *4*, 1992.
[74] T. Da Ros, M. Prato, M. Carano, P. Ceroni, F. Paolucci, S. Roffia, *J. Am. Chem. Soc.* **1998**, *120*, 11645.
[75] P. Cheng, S. R. Wilson, D. I. Schuster, *Chem. Commun.* **1999**, 89.
[76] P. de la Cruz, A. Díaz-Ortiz, J. J. García, M. J. Gómez-Escalonilla, A. de la Hoz, F. Langa, *Tetrahedron Lett.* **1999**, *40*, 1587.
[77] K. A. Jolliffe, S. J. Langford, M. G. Ranasinghe, M. J. Shephard, M. N. Paddon-Row, *J. Org. Chem.* **1999**, *64*, 1238.
[78] K. B. Simonsen, V. V. Konovalov, T. A. Konovalova, T. Kawai, M. P. Cava, L. D. Kispert, R. M. Metzger, J. Becher, *J. Chem. Soc., Perkin Trans. 2* **1999**, 657.
[79] T. Da Ros, M. Prato, D. M. Guldi, E. Alessio, M. Ruzzi, L. Pasimeni, *Chem. Commun.* **1999**, 635.
[80] J.-F. Nierengarten, J.-F. Eckert, J.-F. Nicoud, L. Ouali, V. Krasnikov, G. Hadziioannou, *Chem. Commun.* **1999**, 617.
[81] A. Polese, S. Mondini, A. Bianco, C. Toniolo, G. Scorrano, D. M. Guldi, M. Maggini, *J. Am. Chem. Soc.* **1999**, *121*, 3446.
[82] T. Yamashiro, Y. Aso, T. Otsubo, H. Tang, Y. Harima, K. Yamashita, *Chem. Lett.* **1999**, 443.
[83] M. L. McGlashen, M. E. Blackwood, Jr., T. G. Spiro, *J. Am. Chem. Soc.* **1993**, *115*, 2074.
[84] T. Kato, M. Tachiya, *Chem. Phys. Lett.* **1995**, *241*, 463.
[85] D. M. Guldi, K.-D. Asmus, *J. Am. Chem. Soc.* **1997**, *119*, 5744.
[86] C. Thilgen, A. Herrmann, F. Diederich, *Angew. Chem. Int. Ed. Engl.* **1997**, *36*, 2268.
[87] H. Irngartinger, C.-M. Köhler, G. Baum, D. Fenske, *Liebigs Ann.* **1996**, 1609.
[88] T. Gareis, O. Köthe, J. Daub, *Eur. J. Org. Chem.* **1998**, 1549.
[89] K. Tamaki, H. Imahori, Y. Nishimura, I. Yamazaki, A. Shimomura, T. Okada, Y. Sakata, *Chem. Lett.* **1999**, 227.
[90] Y. Wang, D. I. Schuster, S. R. Wilson, C. J. Welch, *J. Org. Chem.* **1996**, *61*, 5198.
[91] C. Bouden, J.-P. Gisselbrecht, M. Gross, A. Herrmann, M. Rüttimann, J. Crassous, F. Cardullo, L. Echegoyen, F. Diederich, *J. Am. Chem. Soc.* **1998**, *120*, 7860.
[92] F. Diederich, C. Dietrich-Buchecker, J.-F. Nierengarten, J.-P. Sauvage, *J. Chem. Soc., Chem. Commun.* **1995**, 781.
[93] A. I. de Lucas, N. Martín, L. Sánchez, C. Seoane, *Tetrahedron Lett.* **1996**, *37*, 9391.
[94] P. A. Liddell, D. Kuciauskas, J. P. Sumida, B. Nash, D. Nguyen, A. L. Moore, T. A. Moore, D. Gust, *J. Am. Chem. Soc.* **1997**, *119*, 1400.
[95] D. Carbonera, M. D. Valentin, C. Corvaja, G. Agostini, G. Giacometti, P. A. Liddell, D. Kuciauskas, A. L. Moore, T. A. Moore, D. Gust, *J. Am. Chem. Soc.* **1998**, *120*, 4398.
[96] D. Kuciauskas, P. A. Liddell, A. L. Moore, T. A. Moore, D. Gust, *J. Am. Chem. Soc.* **1998**, *120*, 10880.
[97] H. Imahori, K. Yamada, M. Hasegawa, S. Taniguchi, T. Okada, Y. Sakata, *Angew. Chem. Int. Ed. Engl.* **1997**, *36*, 2626.
[98] N. Armaroli, F. Diederich, C. O. Dietrich-Buchecker, L. Flamigni, G. Marconi, J.-F. Nierengarten, J.-P. Sauvage, *Chem. Eur. J.* **1998**, *4*, 406.
[99] D. Armspach, E. C. Constable, F. Diederich, C. E. Housecroft, J.-F. Nierengarten, *Chem. Eur. J.* **1998**, *4*, 723.
[100] S. Higashida, H. Imahori, T. Kaneda, Y. Sakata, *Chem. Lett.* **1998**, 605.
[101] J.-F. Nierengarten, L. Oswald, J.-F. Nicoud, *Chem. Commun.* **1998**, 1545.
[102] J.-F. Nierengarten, C. Schall, J.-F. Nicoud, *Angew. Chem. Int. Ed. Engl.* **1998**, *37*, 1934.
[103] K. Tamaki, H. Imahori, Y. Nishimura, I. Yamazaki, Y. Sakata, *Chem. Commun.* **1999**, 625.
[104] P. Seta, E. Bienvenue, A. L. Moore, P. Mathis, R. V. Bensasson, P. A. Liddell, P. J. Pessiki, A. Joy, T. A. Moore, D. Gust, *Nature* **1985**, *316*, 653.
[105] M. Fujihira, K. Nishiyama, H. Yamada, *Thin Solid Films* **1985**, *132*, 77.
[106] Y. Sakata, H. Tatemitsu, E. Bienvenue, P. Seta, *Chem. Lett.* **1988**, 1625.
[107] M. Fujihira, *Mol. Cryst. Liq. Cryst.* **1990**, *183*, 59.
[108] X. D. Wang, B. W. Zhang, J. W. Bai, Y. Cao, X. R. Xiao, J. M. Xu, *J. Phys. Chem.* **1992**, *96*, 2886.
[109] K. Liang, K.-Y. Law, D. G. Whitten, *J. Phys. Chem. B* **1997**, *101*, 540.
[110] G. Steinberg-Yfrach, P. A. Liddell, S.-C. Hung, A. L. Moore, D. Gust, T. A. Moore, *Nature* **1997**, *385*, 239.
[111] G. Steinberg-Yfrach, J.-L. Rigaud, E. N. Durantini, A. L. Moore, D. Gust, T. A. Moore, *Nature* **1998**, *392*, 479.
[112] A. Ulman (Ed.), *Introduction to Ultrathin Organic Films*, Academic Press, San Diego, **1991**; A. Ulman, *Chem. Rev.* **1996**, *96*, 1533.
[113] T. Akiyama, H. Imahori, A. Ajavakom, Y. Sakata, *Chem. Lett.* **1996**, 907.
[114] H. Imahori, T. Azuma, K. Ushida, M. Takahashi, T. Akiyama, M. Hasegawa, T. Okada, Y. Sakata, *SPIE* **1997**, *3142*, 104.
[115] H. Imahori, S. Ozawa, K. Ushida, M. Takahashi, T. Azuma, A. Ajavakom, T. Akiyama, M. Hasegawa, S. Taniguchi, T. Okada, Y. Sakata, *Bull. Chem. Soc. Jpn.* **1999**, *72*, 485.
[116] T. Akiyama, H. Imahori, Y. Sakata, *Chem. Lett.* **1994**, 1447.
[117] H. Imahori, H. Norieda, S. Ozawa, K. Ushida, H. Yamada, T. Azuma, K. Tamaki, Y. Sakata, *Langmuir* **1998**, *14*, 5335.
[118] H. Imahori, T. Azuma, S. Ozawa, H. Yamada, K. Ushida, A. Ajavakom, H. Norieda, Y. Sakata, *Chem. Commun.* **1999**, 557.
[119] H. Imahori, T. Azuma, A. Ajavakom, H. Norieda, H. Yamada, Y. Sakata, *J. Phys. Chem. B*, in press.
[120] K. C. Hwang, D. Mauzerall, *J. Am. Chem. Soc.* **1992**, *114*, 9705; K. C. Hwang, D. Mauzerall, *Nature* **1993**, *361*, 138; S. Niu, D. Mauzerall, *J. Am. Chem. Soc.* **1996**, *118*, 5791.
[121] C. Luo, C. Huang, L. Gan, D. Zhou, W. Xia, Q. Zhuang, Y. Zhao, Y. Huang, *J. Phys. Chem.* **1996**, *100*, 16685.
[122] H. Imahori, H. Yamada, S. Ozawa, K. Ushida, Y. Sakata, *Chem. Commun.* **1999**, 1165.
[123] M. Fujitsuka, O. Ito, H. Imahori, K. Yamada, H. Yamada, Y. Sakata, *Chem. Lett.* **1999**, 721.
[124] K. Uosaki, T. Kondo, X.-Q. Zhang, M. Yanagida, *J. Am. Chem. Soc.* **1997**, *119*, 8367.
[125] T. Kondo, M. Yanagida, S.-I. Nomura, T. Ito, K. Uosaki, *J. Electroanal. Chem.* **1997**, *438*, 121.

Received April 9, 1999
[O99200]